

AD-A170 219

NUMERICAL SIMULATIONS OF THE CIRCULATION OF THE EASTERN  
MEDITERRANEAN(U) SACLANT ASM RESEARCH CENTRE LA SPEZIA  
(ITALY) D GRILLANI ET AL. NOV 85 SACLANTCEN-SR-92

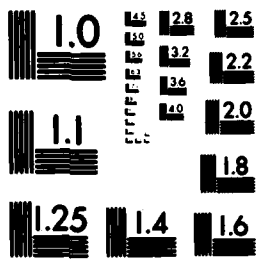
1/1

UNCLASSIFIED

F/G 8/3

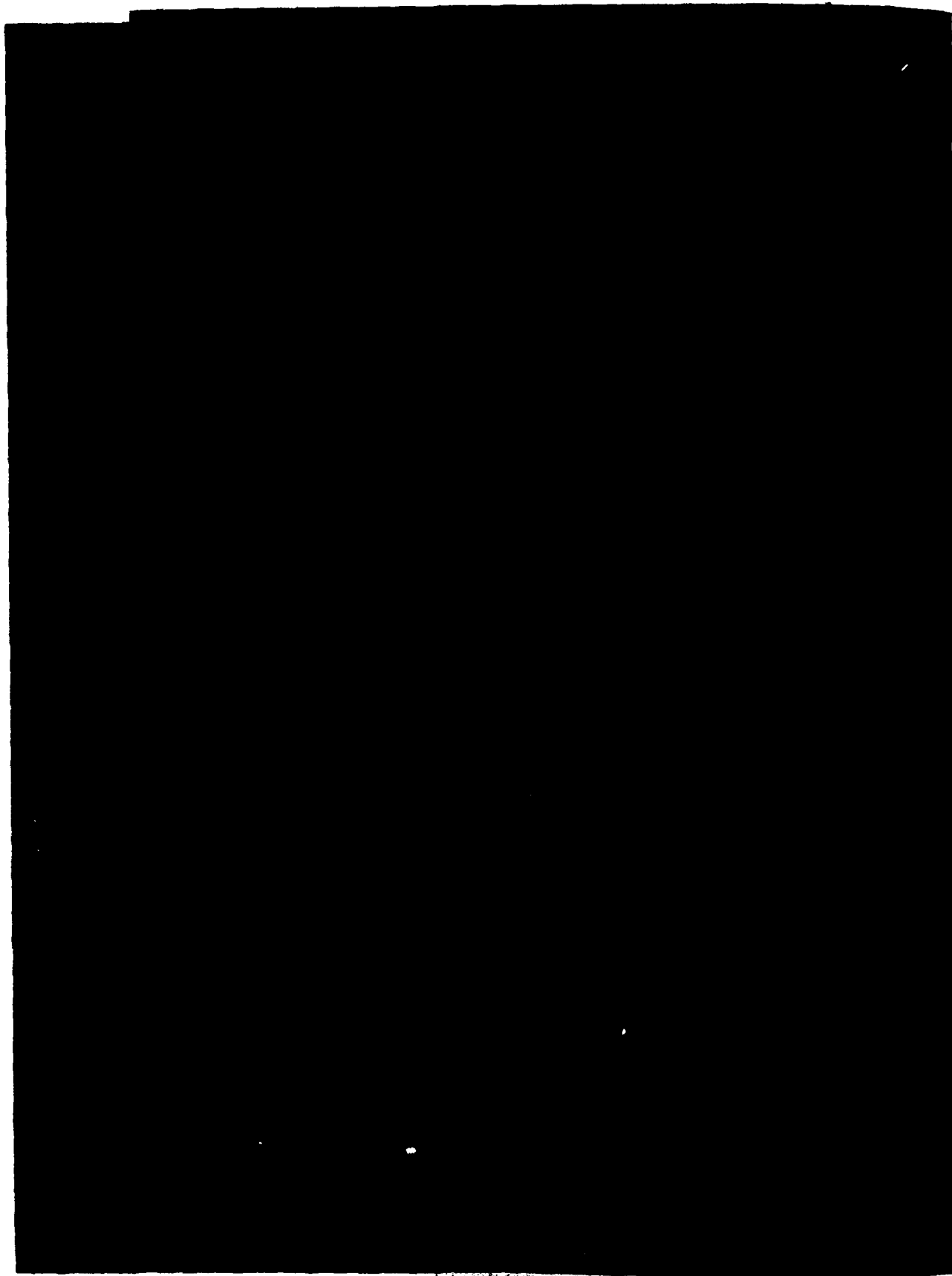
ML

END  
DATE  
8-86  
DTN



MICROCOPY RESOLUTION TEST CHART  
NATIONAL BUREAU OF STANDARDS-1963-A

AD-A170 219



SACLANTCEN REPORT SR-92

NORTH ATLANTIC TREATY ORGANIZATION

SACLANT ASW Research Centre  
Viale San Bartolomeo 400,  
I-19026 San Bartolomeo (SP), Italy.

tel: national 0187 540111  
international + 39 187 540111  
telex: 271148 SACENT I

NUMERICAL SIMULATIONS OF THE CIRCULATION  
OF THE EASTERN MEDITERRANEAN

by

Despina Grillaki  
Steve Piacsek

November 1985

This report has been prepared as part of Project 04.

APPROVED FOR DISTRIBUTION

*Ralph R. Goodman*  
RALPH R. GOODMAN  
Director



B

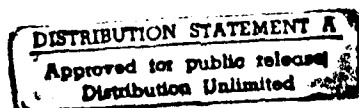


TABLE OF CONTENTS

	<u>Pages</u>
ABSTRACT	1
INTRODUCTION	3
1 THE MODEL	5
2 MODEL RESULTS	9
2.1 Mass transport (Inflow) forcing experiment	9
2.2 Wind forcing experiment	9
2.3 Combined forcing experiment	10
SUMMARY	11
REFERENCES	12

List of Figures

1. a) The Mediterranean and its major seas.	4
b) Surface circulation of the Mediterranean.	4
2. Bathymetry on the eastern Mediterranean sea.	5
3. Solutions of the inflow forces experiment during the fifth year (from January to April).	12
4. Surface layer current flow for December.	13
5. (a) Surface geostrophic components (from observations) of Mediterranean currents in winter.	13
(b) Model results for the wind and inflow forcing case.	13
6. Mean climatological wind stress in a closed basin for January, April, August, November.	14
7. Solutions of wind forcing experiment during the fifth year. (from January to April).	15
8. Solutions of wind forcing experiment during the fifth year. (from May to August).	16
9. Solutions of wind forcing experiment during the fifth year. (from September to December).	17

TABLE OF CONTENTS (cont'd)

<u>List of Figures</u>	<u>Page</u>
10. Velocity field for the wind driven case.	18
11. Solutions of combined wind and inflow forcing experiment during the fifth year (from January to April).	19
12. Solutions of combined wind and inflow forcing experiment during the fifth year (from May to August).	
13. Solutions of combined wind and inflow forcing experiment during the fifth year (from September to December).	21
14. Velocity field for the combined wind and inflow driven case.	22



Accession For		
GEN. GRA&I	<input checked="" type="checkbox"/>	
GEN. TAB	<input type="checkbox"/>	
Announced	<input type="checkbox"/>	
Classification		
<b>PER LETTER ON FILE</b>		
Distribution/		
Availability Codes		
A. J. and/or		
Dist. Special		
<b>A-1</b>		

## NUMERICAL SIMULATIONS OF THE CIRCULATION OF THE EASTERN MEDITERRANEAN

by

Despina Grillaki and Steve Piacsek

ABSTRACT

Oceanographic observations have shown that the surface circulation in the eastern Mediterranean consists of the zonal North African Current along with systems of gyres and rings both north and south of the Current. A large cyclonic gyre occurs between Cyprus and Crete, and another between Greece and Libya. A weaker, quasi-permanent eddy is formed in the Ionian sea and is intensified by the flow through the Strait of Sicily. An anticyclonic ring occurs south of the North African Current in the Gulf of Sirte and another occurs in the southwest Levantine Sea. The reduced-gravity model (one active layer) of Hurlburt and Thompson <6> has been adapted and applied to the semi-enclosed basin of the eastern Mediterranean. Using monthly averages of climatological wind stresses and the estimate of the annual mean flow through the Strait of Sicily, numerical simulations of the circulation in the eastern Mediterranean basin have been carried out. Model runs both with and without inflow through the Straits have been performed. The overall results agree with the observations. They show the presence of the North African Current, two persistent cyclonic gyres of varying strengths and two anticyclonic rings. This modelling effort indicates the importance of the wind induced circulation versus transport for the east-central part of the eastern Mediterranean. It is a first step towards a combined hydrodynamic-thermodynamic model of the circulation in that area.

## INTRODUCTION

This SACLANTCEN report describes a modelling effort that uses realistic geometry, combined forcings, mass transport, and climatology to shed some light on the circulation of the eastern Mediterranean and its driving mechanisms. In particular it discusses the relative importance of wind forcing vis-à-vis inflow-forcing through the Strait of Sicily. The hydrodynamic numerical model simulates the major observed hydrodynamic features of the upper layer circulation, such as meandering currents, persisting gyres and transient eddies.

The Strait of Sicily separates the Mediterranean into western and eastern basins (Fig. 1a). The eastern Mediterranean basin is subdivided into the Adriatic, the Ionian, the Levantine and the Aegean Seas.

The surface circulation in the eastern Mediterranean (Fig. 1b) is significantly influenced by both the Atlantic inflow (originally entering the Mediterranean through the Strait of Gibraltar) and the Levantine basin water. The Atlantic water enters the eastern Mediterranean through the Strait of Sicily (142 km wide, 400 m deep) and forms a slow eastward-flowing surface layer, overriding the sinking, more saline Levantine water that moves westward as an intermediate lower layer <8>.

The Atlantic water has been traced into the eastern Mediterranean by summer observations of a salinity minimum in the upper 25 to 75 m <8>. Modified progressively by evaporation of the surface, the Atlantic water transits the Strait of Sicily, flows along the Libyan and Egyptian coasts and turns along the Israeli coast into the northeast Levantine sea (south of Crete). A series of cyclonic eddies form north of the Current.

A smaller branch of the Atlantic inflow through the Strait of Sicily deflects to the North and is traced into the Ionian sea.

The prevailing westerly winds favour the above circulation pattern. These perennial, relatively strong winds, acting on the limited area of the Mediterranean basin, generate large eddies. These eddies are associated with vertical motions and play an important role in water mass formation by bringing underlying water parcels closer to the mixing regions <4>.

Meteorological forcing and thermodynamics are the main driving physical mechanisms of the eastern Mediterranean. With the help of a simple hydrodynamic model, we have studied the circulation and dynamics of the eastern Mediterranean.

The model consisted of 2-layers, an upper layer 200 m deep and a lower layer of infinite depth. This 'reduced gravity' model has been successfully used in recent years in several studies about the circulation and dynamics of semi-enclosed seas such as the Gulf of Mexico.

PRECEDING PAGE BLANK-NOT FILMED

The recent advances in computer technology have made it possible to run numerical ocean models with sufficient resolution to depict mesoscale ocean features. The most extensive study along these lines was done by Hurlburt and Thompson <6>, in which they successfully simulated many dynamic features of the loop current in the Gulf of Mexico.

More relevant to this work in the Mediterranean were the modelling studies of Preller and Hurlburt <12> and Preller <13> for the Alboran Sea and Preller and Heburn <14> for the western Mediterranean Sea. The western Mediterranean study also used realistic geometry and bottom topography, and combined forcings from the Strait of Gibraltar inflow and monthly averaged wind stresses.

As for the eastern Mediterranean, one earlier study <14> used the reduced-gravity model with an idealized rectangular basin geometry. Another eastern Mediterranean study (unpublished) uses a two-layer active 'rigid lid' model (i.e. assumes a level surface). Both of these studies simulated only the wind-driven circulation.

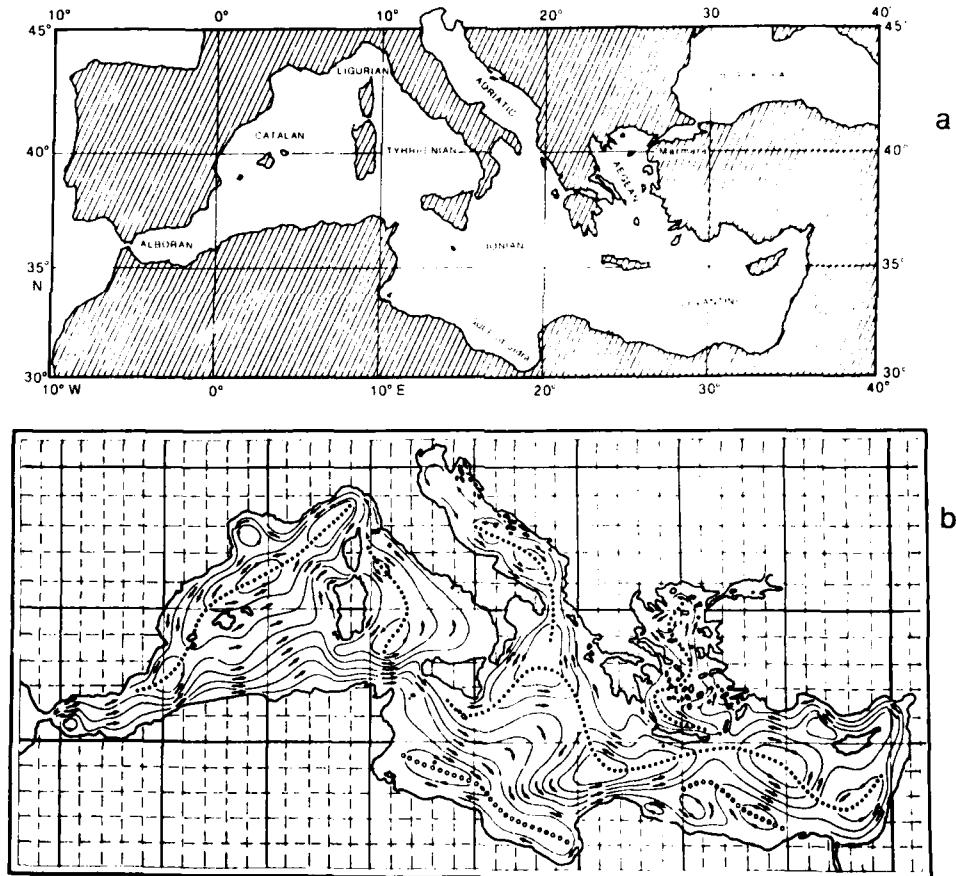


FIG. 1 a) THE MEDITERRANEAN AND ITS MAJOR SEAS.  
b) SURFACE CIRCULATION OF THE MEDITERRANEAN.

1 THE MODEL

The numerical model used in this study of the eastern Mediterranean has been modified and adapted from one developed for the Gulf of Mexico <6>.

The model is an active upper layer, hydrodynamic model on a b-plane. The model, of the first baroclinic mode, exclude baroclinic instability and assumes Boussinesq approximation. Such models are known as 'reduced-gravity models' because the effective gravity acting on the active upper layer is reduced by the density ratio,

$$g' = g(\Delta\rho / \rho) \quad (\text{Eq. 1})$$

and

$$\rho_1 - \rho_2 / \rho \quad , \quad (\text{Eq. 2})$$

where

$g$  is acceleration due to gravity and  
 $\rho$  is the density.

The active upper layer is 200 m deep and the static lower layer is infinitely deep; between them is an impermeable interface. The model uses realistic irregular geometry (coastline), Fig. 2, drawn from the Synthetic Bathymetric Profiling System (SYNBAPS) of Vanwyckhouse <15, 16>.

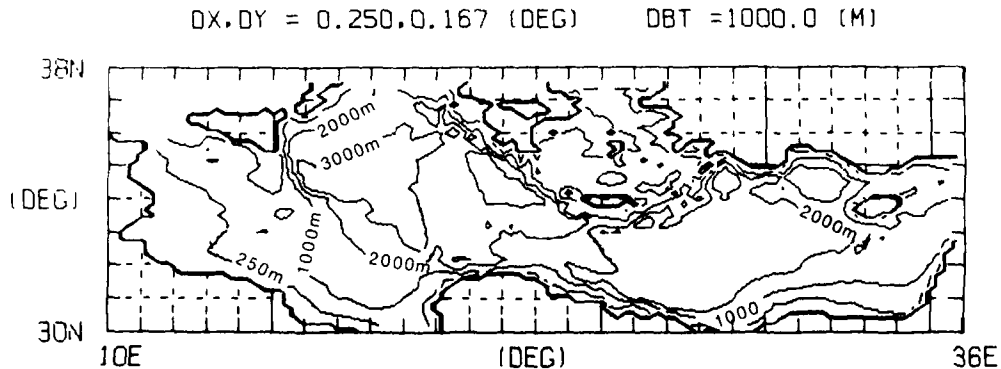


FIG. 2 BATHYMETRY ON THE EASTERN MEDITERRANEAN SEA  
 (from SYNBARS data).

The grid resolution is 1/4 of a degree (21.4 km in the east-west direction) and 1/6 of a degree (18.6 km in the north-south direction). The fine grid resolution allows the study of mesoscale features.

The model domain extends from 10° to 36°E longitude and from 30° to 38°N latitude. For the coastline a cut-off depth of 20 m was used in order to eliminate errors existing at the boundary of the data set. Except at the ports, the boundaries are rigid with a no-slip boundary condition. The inflow transport values are based on observations.

The vertically integrated equations used in the model are the equation of motion (Eq. 1), including pressure, Coriolis acceleration, wind stress and frictional terms, and the equation of continuity (Eq. 2). They are:

$$\frac{\partial \vec{V}_1}{\partial t} + (\nabla \cdot \vec{V}_1 + \vec{V}_1 \cdot \nabla) \vec{V}_1 + \hat{K} \times f \vec{V}_1 = -h_1 \nabla P_1 + \rho^{-1} (\vec{T}_1 - \vec{T}_2) + A \nabla^2 \vec{V}_1 \quad (\text{Eq. 3})$$

$$\frac{\partial h_1}{\partial t} + \nabla \cdot \vec{V}_1 = 0 \quad (\text{Eq. 4})$$

where

$$\nabla = \frac{\partial}{\partial x} \hat{i} + \frac{\partial}{\partial y} \hat{j} ,$$

$$P_1 = g h_1 ,$$

$$\vec{V}_1 = h_1 \vec{v}_1 = h_1 (u_1 \hat{i} + v_1 \hat{j}) ,$$

$$g' = g(\rho_2 - \rho_1) \rho^{-1} ,$$

$$f = f_0 + \beta(y - y_0) ,$$

and

$$\vec{T}_1 = T_1(x) \hat{i} + T_1(y) \hat{j} .$$

$x$  and  $y$  are tangent-plane Cartesian coordinates,  $u_1$  and  $v_1$  are the eastward and northward velocity components in the upper layer,  $h_1$  is the upper layer thickness,  $t$  is the time,  $g$  is the acceleration due to gravity,  $\rho_i$  is the density of seawater in layer  $i$ ,  $f_0$  and  $Y_0$  are the values of the Coriolis force, and the  $y$ -coordinate at the southern boundary,  $T_x$  is the wind stress, and  $T_y$  is the interfacial stress. The remaining parameters are defined in Table 1.

TABLE 1  
MODEL PARAMETERS

PARAMETER	DEFINITION	VALUE
A	Eddy viscosity	$1000 \text{ m}^2 \text{ s}^{-1}$
b	(Df/Dy)	$1.8 \times 10^{-11} \text{ m}^{-1} \text{ s}^{-1}$
f <sub>0</sub>	Coriolis parameter	$8 \times 10^{-5} \text{ s}^{-1}$
g'	Reduced gravity due to stratification	$0.02 \text{ m s}^{-2}$
h <sub>1</sub>	Undisturbed upper layer depth	200 m
L <sub>x</sub>	East-west dimension of the model domain	10°E to 36°E longitude
L <sub>y</sub>	North-south dimension of the model domain	30°N to 38°N latitude
x, y	Horizontal grid resolution	21.4 km (1/4°) × 18.6 km (1/6°)
t	Time step	2700 s
V <sub>in</sub>	Inflow velocity	5 cm s <sup>-1</sup>
T <sub>sin</sub>	Inflow spin up time constant	30 days
T <sub>swind</sub>	Wind spin up time constant	2 days
α	Angle of inf'ow (Strait of Sicily)	135°

Inflow is exactly balanced by outflow through an open eastern boundary (port). This is accomplished by allowing normal flow at the eastern boundary to be self-determined and by imposing an integral constraint on total mass outflow.

The model parameters and their values are given in Table 1. The value for the eddy viscosity was chosen to keep the Reynolds number low for computational stability. The value of the reduced gravity coefficient is the average density difference of the Mediterranean environment at these levels. The undisturbed upper layer depth value generally represents the upper end of the thermocline and was derived from observations.

The inflow velocity is spun up over a period of thirty days to minimize the excitation of high frequency waves. The winds have a shorter spin up period of two days.

The inflow port representing the Strait of Sicily is defined by 5 grid points and is 142 km wide. The artificial outflow port accounting for the evaporation and sinking of waters into greater depths is also defined by 5 grid points but is 93 km wide. An inflow velocity of 5 cm/s corresponds to a transport of  $0.96 \times 10^6 \text{ m}^3/\text{s}$  (0.96 Sv) through the Straits of Sicily, which agrees with observations <2, 3>.

The direction of the inflow is taken as  $135^\circ$ . The inflow is independent of time and represents only the mean annual flux. Its temporal and spatial variations in the Strait of Sicily are assumed to balance out, i.e. no net change. However, in reality, the Atlantic water travels by spreading laterally and is seasonally dependent.

The open eastern boundary condition outflow port accounts for the evaporation and the sinking of surface waters and therefore satisfies the equation of continuity.

The outflow port location was chosen near the Israeli coast as a first attempt to approach the observed oceanographic circulation patterns. The model results have shown that the outflow port location was not an important factor for this study. The Atlantic origin water sinks in the northeast Levantine Sea and, in the Crete-Rhodes-Cyprus area, is transformed into the denser Intermediate Mediterranean water. In winter the surface atmospheric fluxes enhance the vertical circulation which accompanies the formation of the Intermediate Mediterranean water.

The monthly climatological wind forcing has been derived from twenty years of ship observations <9>. These monthly averages of wind stresses are computed on a  $1^\circ$  latitude  $\times$   $1^\circ$  longitude (Marsden Square) grid. When applied to the  $1/4^\circ$  by  $1/6^\circ$  model grid, the winds are bilinearly interpolated.

## 2 MODEL RESULTS

The model was subjected to a series of experiments to determine the influence of mass transport and wind forcings, singly or in combination, on surface circulation.

Firstly, the model was forced only by mass transport through the Strait of Sicily to examine the contribution to the surface circulation. Secondly, the model was forced by monthly climatological wind stress to examine the purely wind-driven circulation. Thirdly, a combination of transport and wind stress forcings were applied.

### 2.1 Mass transport (Inflow) forcing experiment

The experiment has been integrated over five years. The results are presented (Figs. 3, 4) in terms of pycnocline height deviation of the interface between the upper and lower layers and current patterns. (The pycnocline height deviation is the deviation of the interface from its rest position of 200 m). Figure 3 presents results for January, February, March and April for the 5<sup>th</sup> year of simulation. Figure 4 shows the current pattern of the active upper layer for the month of December.

With inflow forcing alone, the Atlantic origin water passes through the Strait of Sicily, and flows along the African coast as an extension of the North African Current. Little difference is observed between figures, thus indicating the existence of a steady state.

No seasonal changes are found in the circulation patterns. However, the effects of changes in direction and velocity of the inflow do affect the path of the current, as in the Alboran sea <12> but this effect was not studied. The flow-channel of the Strait of Sicily is oriented such that the entering current flows southward directing the mass transport close to the North African coast.

Compared to observational data <10, 11>, the model indicates only the North African Current with very low speeds and an absence of gyres and of circulation in the northern part of the basin (Fig. 5). Because the inflow alone represents only a minor contribution to the east Mediterranean circulation, the variations in inflow and the outflow port location were not important for this particular study.

### 2.2 Wind forcing experiment

In this experiment the ports are closed and the wind stresses (analyzed by May <9>) blow over the eastern part of the basin. Thus the solutions

(Fig. 6) represent circulation due only to climatological wind stress applied in a closed basin. Figures 7, 8, 9 show monthly solutions for the fifth year of integration in terms of the pycnocline anomaly and Fig. 10 shows the current pattern of the active upper layer for the month of December.

In the central part of the eastern basin several persistent gyres appear along with a strong cyclonic circulation. Cyclonic gyres persist between southern Greece and Libya and between Cyprus and Crete. Also a permanent anticyclonic gyre appears in the southwest Levantine basin.

For the western part of the eastern Mediterranean basin the circulation pattern varies seasonally. The North African Current appears in the solution. A cyclonic quasi-steady eddy appears in the Ionian Sea and a seasonal anticyclonic gyre appears in the Gulf of Sirte.

Model solutions show monthly and seasonal variation of circulation with an maximum in winter and a minimum in late summer. However, the Aegean is an exception; here the maximum occurs in late summer. The magnitudes of the wind stresses (Fig. 6) also show an overall maximum in the winter with the exception of the Aegean Sea, where the maximum occurs in late summer. (These strong northern summer winds are called the Etesians.) May <9> has determined large wind stress values in the area of the two major cyclonic gyres formed east and west of Crete.

The model results compare well with the observational data (Fig. 5) in the central and eastern parts of the basin but give less consistent all year around results for the western part. The results indicate that the wind stress, as a driving force, is responsible for the development of the major cyclonic gyres throughout the year.

### 2.3 Combined forcing experiment

This experiment consisted of combining the mass transport through the Strait of Sicily with the wind driven experiment at the end of the fifth year. Then this combination was run for five more years. This approach was used because the inflow-forced solutions reach a steady state more quickly than the wind-forced ones.

Figures 11 to 14 represent the model solution and resemble a superposition of the two previously examined independent cases. Several results are apparent: the inflow seems to intensify both the semi-permanent eddy in the northwestern basin and the anticyclonic ring in the Gulf of Sirte, which now becomes permanent throughout the year. The North African Current appears at the south of the basin. In the eastern basin the cyclonic gyres between Cyprus and Crete and between Greece and Libya are still maintained as is the anticyclonic ring in the southwest Levantine Sea. The intensity of the features seems to grow stronger in late winter and early spring.

The model agrees well with Ovchinnikov's observations <10, 11>. Both the observations and the model present cyclonic gyres north of the North African Current and anticyclonic rings south of it.

The similarity between the modelled (see Fig. 5) and the observed circulation patterns is stronger for the eastern and central part of the basin than for the western part. The implication is that the wind, rather than inflow, is the dominant physical influence on the surface patterns.

For the western part of the basin the restricted domain of the model and the driving forces, i.e. mass transport and wind stress, have only a limited capability to describe the surface circulation. The modelling experiments also show that the inflow represents only a minor contribution to the eastern Mediterranean circulation.

#### SUMMARY

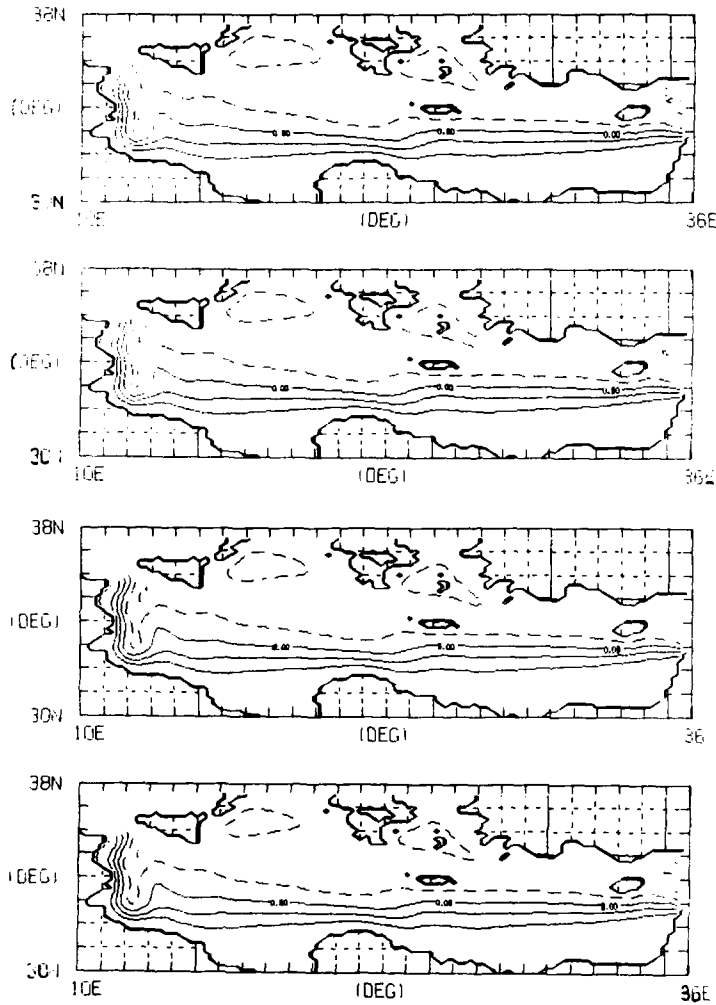
The surface circulation of the Mediterranean east of the Strait of Sicily has been described by a simple, one (active) layer, reduced-gravity model. Although this model doesn't consider bottom topography, thermodynamics, or mixing (except for lateral diffusion of momentum), it has produced a first approximation to the mass transport through the Strait of Sicily and the seasonally varying climatological wind stresses. The modelling experiments first determined the influence of mass transport on surface circulation. This was followed by experiments to determine the influence of wind stress. Finally, the modelling experiments considered a combination of both factors.

The overall results showed a qualitative agreement with Ovchinnikov <10, 11> observed winter circulation patterns in this area. The North African Current, two major cyclonic gyres and a seasonal eddy to the north and two anticyclonic rings to the south, observed in the circulation patterns, appear also in the model. However, they differ in the intensity of circulation and the location of the gyre centers. In the model, the large gyres, east and west of Crete, are centered much closer to the island than indicated by the observed results. The ring in the southwest Levantine basin is more distant from the coast in the model than in the observed results.

The model creates a realistic large scale surface circulation pattern. Wind-induced circulation is an important physical mechanism for influence of the circulation in the central and eastern parts of the eastern Mediterranean. Mass transport is only a minor influence except in the function of the North African Current.

This report presents preliminary results of experiments to model the circulation of the eastern Mediterranean. Additional hydrodynamic computations are needed to improve the model. These should include the time dependence of the inflow through the Strait of Sicily and should employ a two (active) layer model to account for the subsurface outflow and bottom topography. A more complete numerical simulation of the circulation in the eastern Mediterranean should consider thermodynamics and use more realistic wind forcing functions.

INTERFACE DEVIATIONS



**a**

DAY = 1470  
 DH = 5.0 (m)  
 MIN = -1.05E+01  
 MAX = 1.52E+01

**b**

DAY = 1500  
 DH = 5.0 (m)  
 MIN = -1.06E+01  
 MAX = 1.53E+01

**c**

DAY = 1530  
 DH = 5.0 (m)  
 MIN = -1.04E+01  
 MAX = 1.53E+01

**d**

DAY = 1560  
 DH = 5.0 (m)  
 MIN = -1.07E+01  
 MAX = 1.53E+01

FIG. 3 SOLUTIONS OF THE INFLOW FORCES EXPERIMENT DURING THE FIFTH YEAR.

(a) January (c) March  
 (b) February (d) April

Solid contours indicate deepening of the interface and anticyclonic circulation; dashed contours indicate shallowing and cyclonic circulation.

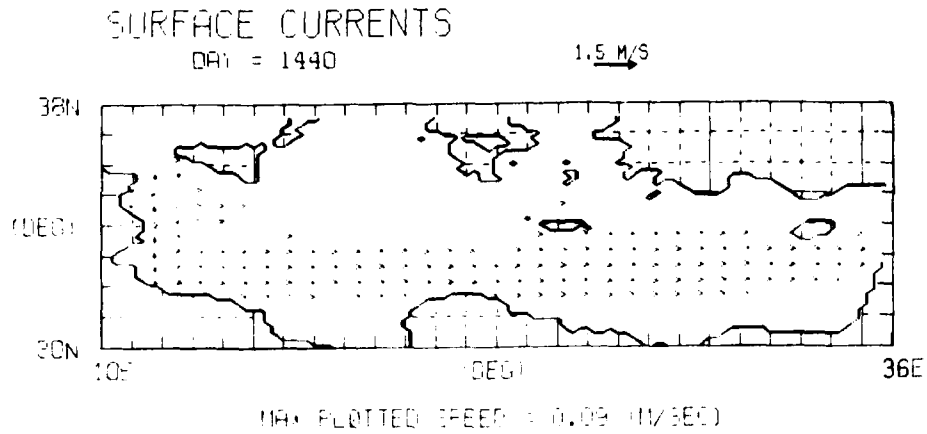


FIG. 4 SURFACE LAYER CURRENT FLOW FOR DECEMBER  
(Inflow driven case).

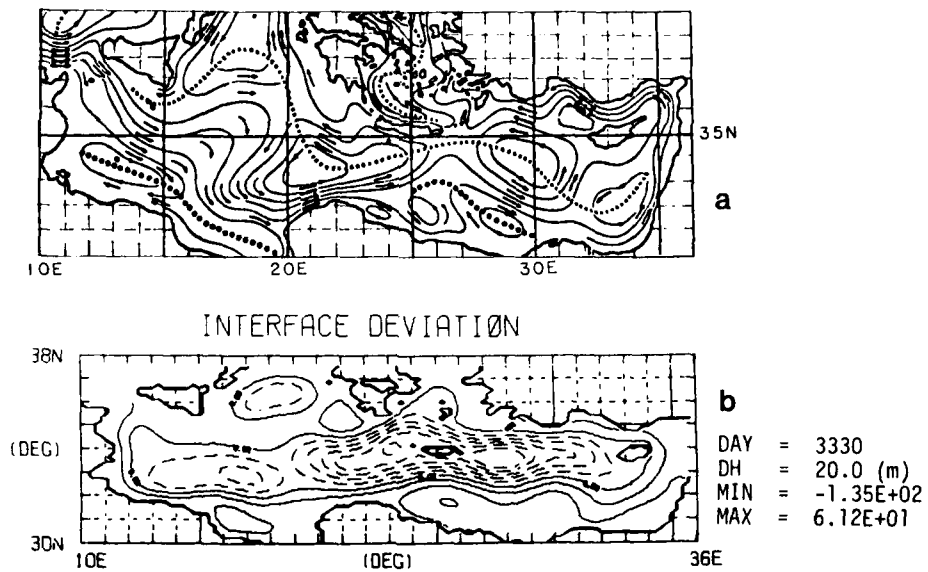
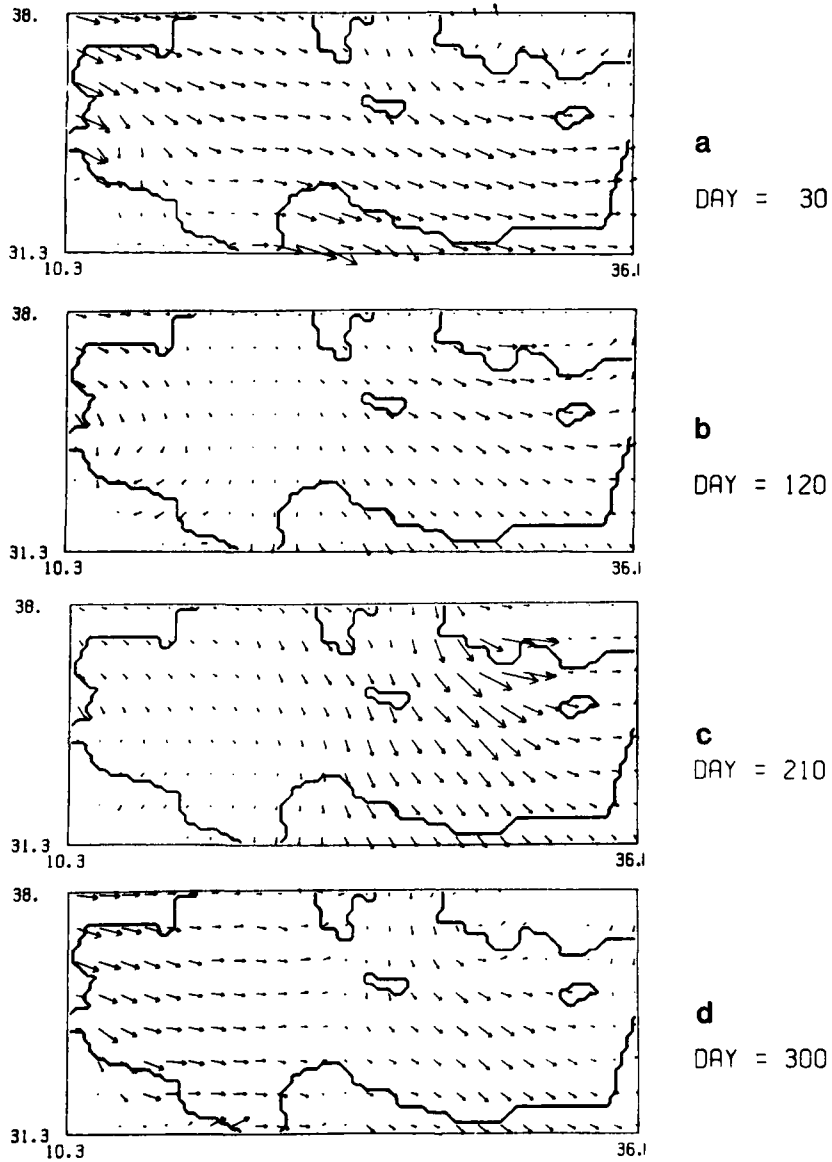
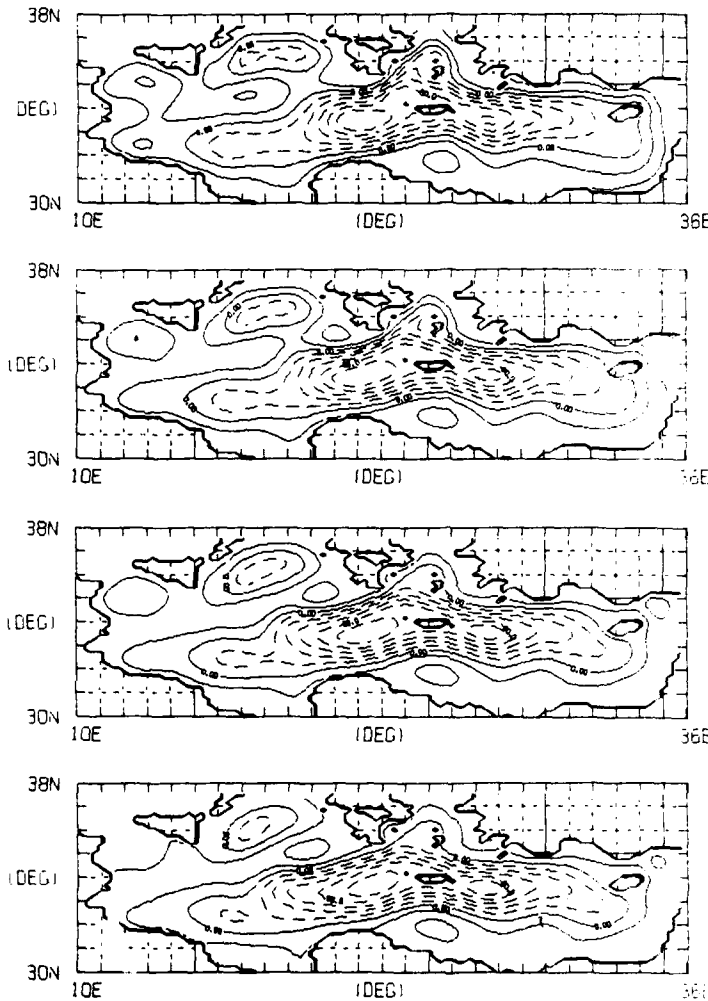


FIG. 5 (a) SURFACE GEOSTROPHIC COMPONENTS (FROM OBSERVATIONS) OF  
MEDITERRANEAN CURRENTS IN WINTER.  
(b) MODEL RESULTS FOR THE WIND AND INFLOW FORCING CASE.



**FIG. 6** MEAN CLIMATOLOGICAL WIND STRESS IN A CLOSED BASIN FOR  
(a) January (c) August  
(b) April (d) November  
The lengths of the arrows are proportional to wind stress magnitude.

INTERFACE DEVIATIONS



**a**

DAY = 1470  
 DH = 20.0 (m)  
 MIN = -1.31E+02  
 MAX = 4.73E+01

**b**

DAY = 1500  
 DH = 20.0 (m)  
 MIN = -1.20E+02  
 MAX = 4.80E+01

**c**

DAY = 1530  
 DH = 20.0 (m)  
 MIN = -1.16E+02  
 MAX = 4.94E+01

**d**

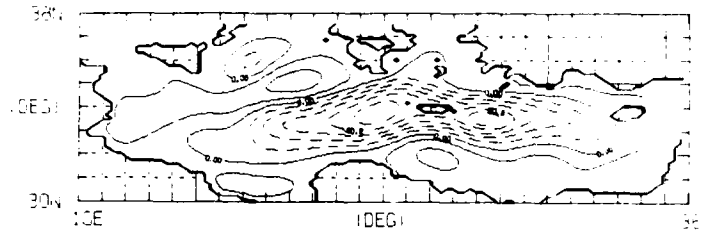
DAY = 1560  
 DH = 20.0 (m)  
 MIN = -1.16E+02  
 MAX = 4.97E+01

FIG. 7 SOLUTIONS OF WIND FORCING EXPERIMENT DURING THE FIFTH YEAR.

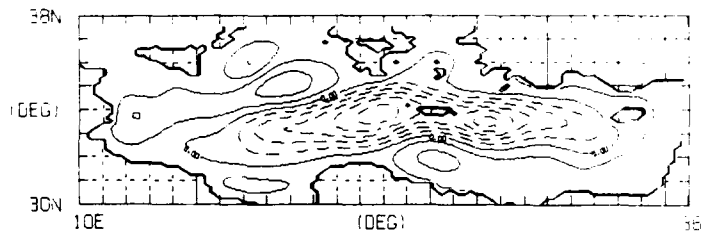
(a) January (c) March  
 (b) February (d) April

Solid contours indicate deepening of the interface and anticyclonic circulation; dashed contours indicate shallowing and cyclonic circulation.

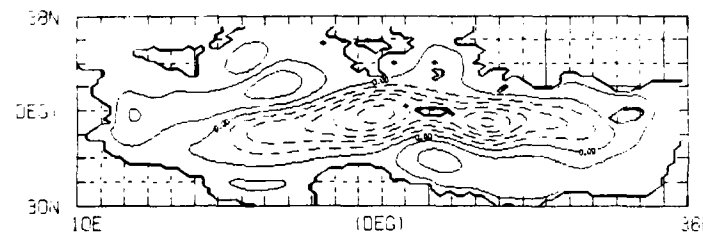
INTERFACE DEVIATIONS



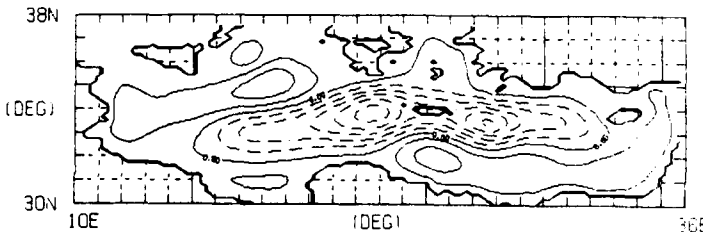
**a**  
 DAY = 1590  
 DH = 20.0 (m)  
 MIN = -1.14E+02  
 MAX = 5.07E+01



**b**  
 DAY = 1620  
 DH = 20.0 (m)  
 MIN = -1.11E+02  
 MAX = 5.29E+01



**c**  
 DAY = 1650  
 DH = 20.0 (m)  
 MIN = -1.10E+02  
 MAX = 5.50E+01



**d**  
 DAY = 1680  
 DH = 20.0 (m)  
 MIN = -1.11E+02  
 MAX = 5.58E+01

FIG. 8 SOLUTIONS OF WIND FORCING EXPERIMENT DURING THE FIFTH YEAR.

(a) May (c) July  
 (b) June (d) August

Solid contours indicate deepening of the interface and anticyclonic circulation; dashed contours indicate shallowing and cyclonic circulation.

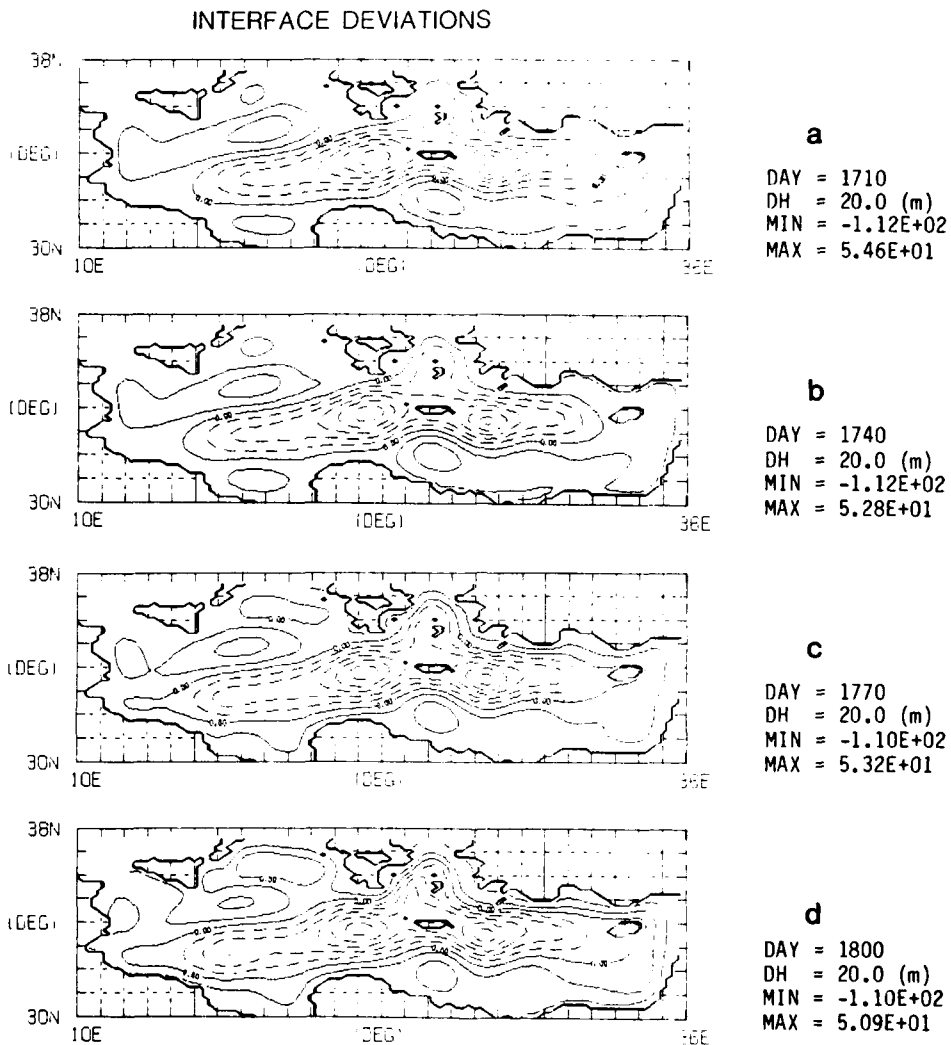


**FIG. 9 SOLUTIONS OF WIND FORCING EXPERIMENT DURING THE FIFTH YEAR.**  
 (a) September (c) November  
 (b) October (d) December  
 Solid contours indicate deepening of the interface and anticyclonic circulation; dashed contours indicate shallowing and cyclonic circulation.

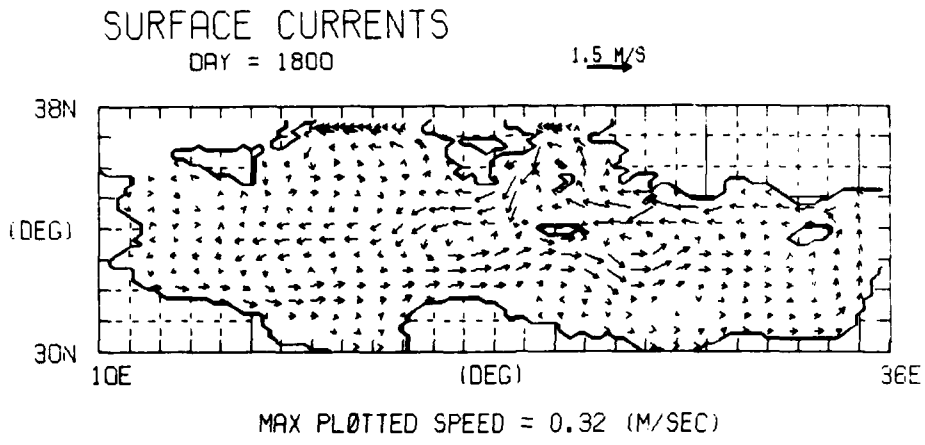
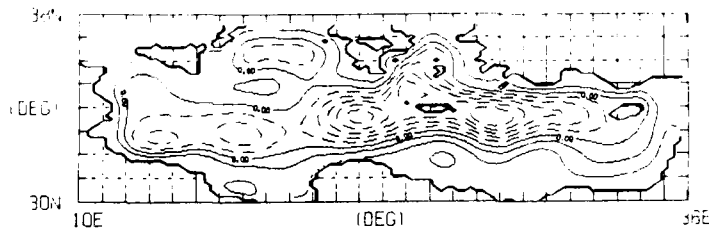


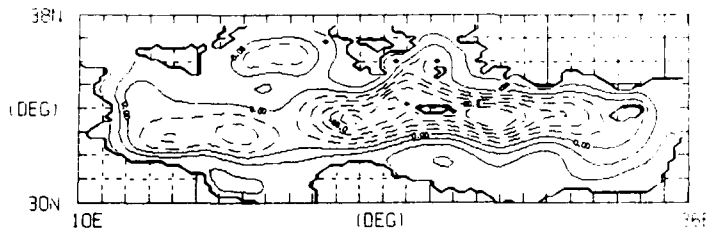
FIG. 10 VELOCITY FIELD FOR THE WIND DRIVEN CASE.

INTERFACE DEVIATIONS



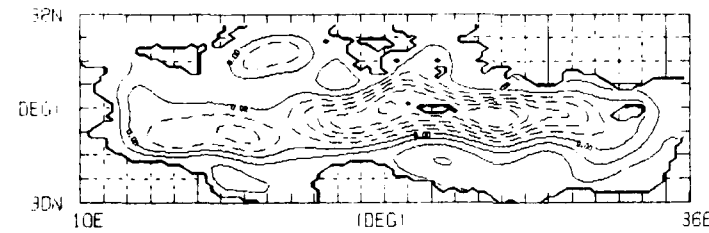
**a**

DAY = 3270  
 DH = 20.0 (m)  
 MIN = -1.24E+02  
 MAX = 6.32E+01



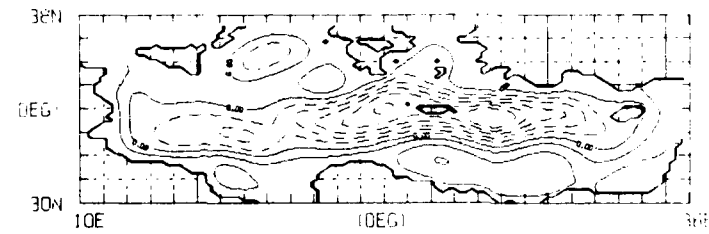
**b**

DAY = 3300  
 DH = 20.0 (m)  
 MIN = -1.32E+02  
 MAX = 6.18E+01



**c**

DAY = 3330  
 DH = 20.0 (m)  
 MIN = -1.35E+02  
 MAX = 6.12E+01



**d**

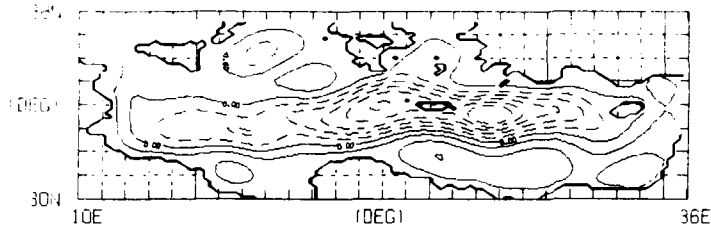
DAY = 3360  
 DH = 20.0 (m)  
 MIN = -1.35E+02  
 MAX = 6.08E+01

FIG. 11 SOLUTIONS OF COMBINED WIND AND INFLOW FORCING EXPERIMENT DURING THE FIFTH YEAR.

(a) January (c) March  
 (b) February (d) April

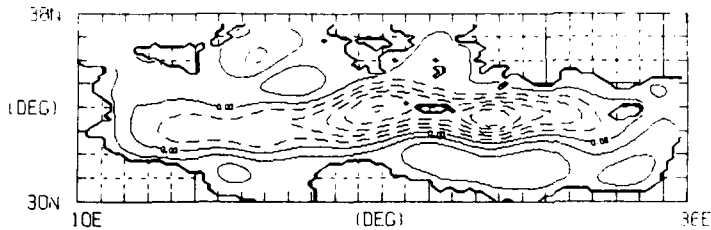
Solid contours indicate deepening of the interface and anticyclonic circulation; dashed contours indicate shallowing and cyclonic circulation.

INTERFACE DEVIATIONS



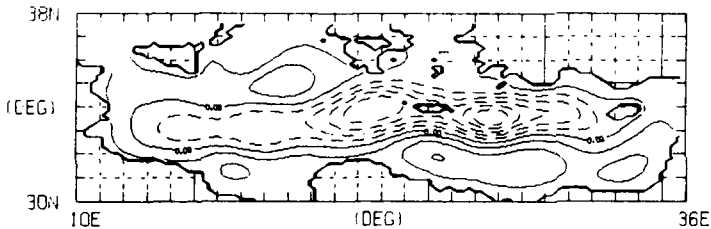
**a**

DAY = 3390  
 DH = 20.0 (m)  
 MIN = -1.31E+02  
 MAX = 6.02E+01



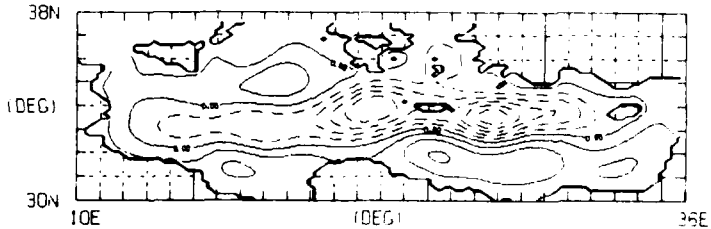
**b**

DAY = 3420  
 DH = 20.0 (m)  
 MIN = -1.26E+02  
 MAX = 6.00E+01



**c**

DAY = 3450  
 DH = 20.0 (m)  
 MIN = -1.21E+02  
 MAX = 6.09E+01



**d**

DAY = 3480  
 DH = 20.0 (m)  
 MIN = -1.18E+02  
 MAX = 6.24E+01

**FIG. 12 SOLUTIONS OF COMBINED WIND AND INFLOW FORCING EXPERIMENT DURING THE FIFTH YEAR.**  
 (a) May (c) July  
 (b) June (d) August  
 Solid contours indicate deepening of the interface and anticyclonic circulation; dashed contours indicate shallowing and cyclonic circulation.

INTERFACE DEVIATIONS

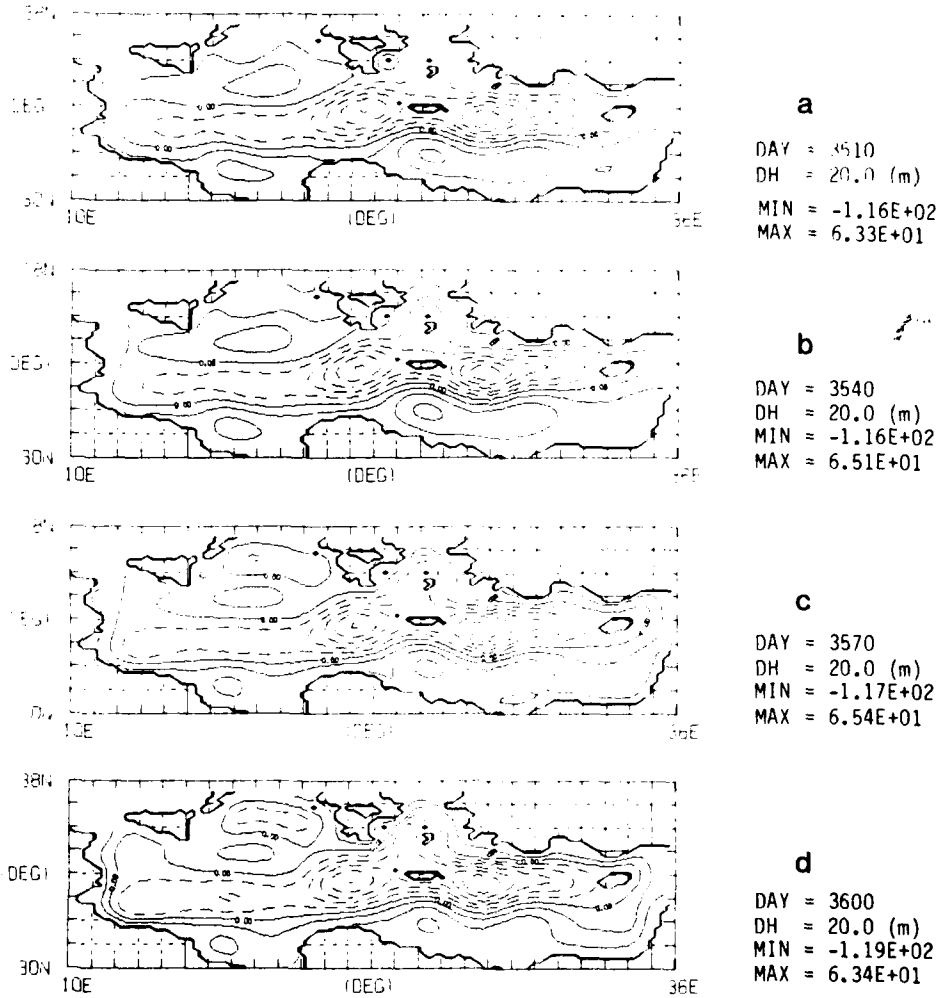


FIG. 13 SOLUTIONS OF COMBINED WIND AND INFLOW FORCING EXPERIMENT DURING THE FIFTH YEAR.

(a) September (c) November  
 (b) October (d) December

Solid contours indicate deepening of the interface and anticyclonic circulation; dashed contours indicate shallowing and cyclonic circulation.

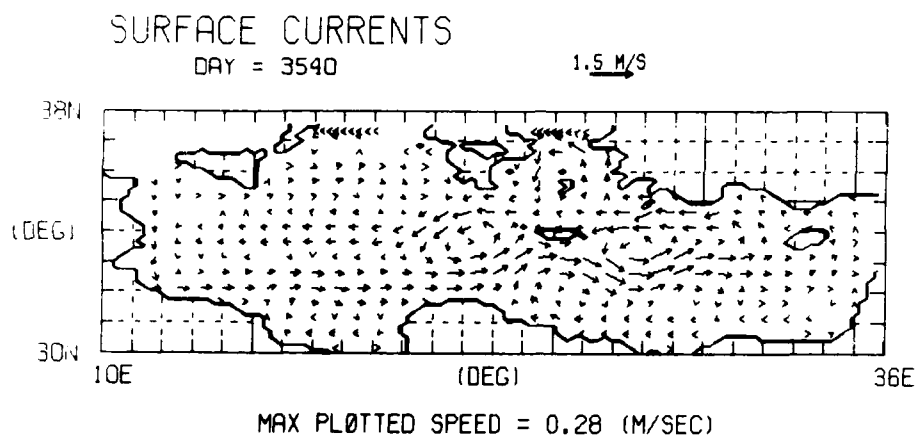


FIG. 14 VELOCITY FIELD FOR THE COMBINED WIND AND INFLOW DRIVEN CASE.

REFERENCES

1. ALLAIN, C. Topographie dynamique. Revue des Travaux de l'Institut des Pêches Maritimes, 24, 1960: 121-137.
2. BETHOUX, J.P. Budgets of the Mediterranean Sea. Their dependence on the local climate and on the characteristics of the Atlantic waters. Oceanologica Acta 2, 1979:157-163.
3. GARZOLI, S. and MAILLARD, C. Winter circulation in the Sicily and Sardinia Straits region, Deep Sea Research, 26, 1979: 933-954.
4. GASCARD, J.-C. Vertical motions in a region of deep water formation. Deep Sea Research, 20, 1973: 1011-1027.
5. GRILLAKI, D, and PIACSEK, S. Numerical simulations of the circulation of the Eastern Mediterranean, Terra Cognita, 4, 1984: 334-335.
6. HURLBURT, H.E. and THOMPSON, J.D. A numerical study of loop current intrusions and eddy shedding. Journal of Physical Oceanography, 10, 1980: 1611-1651.
7. LACOMBE, H. and TCHERNIA, P. Quelques traits généraux de l'hydrologie Méditerranéenne d'après diverses campagnes hydrologiques récentes en Méditerranée dans le proche Atlantique et dans le détroit de Gibraltar. Cahiers Océanographiques, 12, 1960: 527-547.
8. LACOMBE, H. and TCHERNIA, P. Caractères Hydrologiques et Circulation des eaux en Méditerranée. In: STANLEY, D.J., ed. The Mediterranean Sea: a Natural Sedimentation Laboratory. Stroudsburg, PA, Dowden, 1973: pp. 25-36.
9. MAY, P.W. Climatological flux estimates in the Mediterranean Sea: part I. Winds and wind stress, NORDA TR-54. NSTL Station, MS, Naval Ocean Research and Development Activity, 1982.
10. OVCHINNIKOV, I.M. Circulation in the surface and intermediate layers of the Mediterranean. Oceanology, 6, 1966: 48-59.
11. OVCHINNIKOV, I.M. On the water balance of the Mediterranean sea. Oceanology, 14, 1974: 198-202.
12. PRELLER, R. and HURLBURT, H.E. A reduced gravity model of circulation in the Alboran sea. In: NIHOUL, J.C., ed. Hydrodynamics of semi-enclosed seas. Amsterdam, Elsevier, 1982: pp. 75-90.

13. PRELLER, R. A numerical model of circulation in the Alboran Sea. PHD Thesis, 1984, Florida State University.
14. PRELLER, R. and HEBURN, G. A simple numerical model of circulation in the western Mediterranean sea. Submitted to Oceanologica Acta, 1984.
15. VANWYCKHOUSE, R.J. Synthetic bathymetric profiling system (SYNBAPS), TR 233, Washington, D.C., Naval Oceanographic Office, 1973.
16. VANWYCKHOUSE, R.J. SYNBAPS, volume I: Data sources and data preparation, NORDA TN 35, NSTL Station, MS, Naval Ocean Research and Development Activity, 1979.

KEYWORDS

ANTICYCLONIC  
APRIL  
AUGUST  
CIRCULATION  
CLIMATOLOGY  
CORIOLIS ACCELERATION  
CORIOLIS FORCE  
CRETE  
CURRENT  
CYCLONIC  
CYPRUS  
DECEMBER  
EASTERN MEDITERRANEAN  
EDDY  
EVAPORATION  
FEBRUARY  
FORCING  
GEOSTROPHIC  
GREECE  
GULF OF SIRTE  
GYRES  
HYDRODYNAMICS  
INFLOW  
IONIAN SEA  
JANUARY  
JULY  
JUNE  
LEVANTINE SEA  
LIBYA  
LOWER LAYER  
MARCH  
MASS TRANSPORT  
MAY  
MODEL  
NORTH AFRICAN CURRENT  
NOVEMBER  
OCTOBER  
REDUCED GRAVITY MODEL  
SALINITY  
SEPTEMBER  
SIMULATION  
STRAIT OF SICILY  
SURFACE  
SYNBAPS  
SYNTHETIC BATHYMETRY PROFILING SYSTEM  
UPPER LAYER  
WIND  
WINTER

END

DATE  
FILMED

8-86

DTIC